Analytical Subdomain Model of Surface-Mounted PM Synchronous Machine Using Virtual PM Blocks to Optimize Magnet Segmentations for Underwater Vehicle Applications

Tow Leong Tiang, Dahaman Ishak and Mohamad Kamarol

Abstract This paper presents an analytical subdomain model which can consider infinite numbers of virtual permanent magnet (PM) blocks to represent the segmented magnets per pole in any combination of slot and pole numbers of the semi-closed surface-mounted permanent magnet synchronous machines. From the case study discussed in this paper for a three-phase, 6 s/4p surface-mounted PMSM designed specifically for the underwater vehicle applications, the optimum magnet pole-arcs of the two segmented magnets per pole are 147.0° elect. for each magnet pole and 11.3° elect. for the airgap spacing between the magnet segments. The cogging torque and the total harmonic distortion of the phase back-EMF are drastically reduced by 88 % and 26 %, respectively, when comparing the results to the optimum magnet pole-arc of one magnet segment per pole machine, under similar constraint of PM volume. These analytical results are validated by 2D finite element analysis, where good agreement has been achieved.

Keywords Analytical · Subdomain model · Permanent magnet · Synchronous machines · Magnet segmentation

T.L. Tiang (✉) · D. Ishak · M. Kamarol
School of Electrical and Electronic Engineering, Universiti Sains Malaysia, 14300 Nibong Tebal, Penang, Malaysia
e-mail: TL.Tiang.ee@gmail.com

D. Ishak
e-mail: dahaman@usm.my

M. Kamarol
e-mail: eekamarol@usm.my

H. Ibrahim et al. (eds.), *9th International Conference on Robotic, Vision, Signal Processing and Power Applications*, Lecture Notes in Electrical Engineering 398,
DOI 10.1007/978-981-10-1721-6_91

1 Introduction

Compared to the traditional electric machines, permanent magnet synchronous machines (PMSMs) are more favorable in the servo drives and propulsion systems, especially designed for the underwater vehicles (UVs) owing to its higher efficiency and higher torque density. However, the optimum dimension of PMSMs should be determined properly during preliminary designing stage in order to mitigate the torque ripples. In the past research, different topologies of PMSMs have been proposed as the prime mover of UVs, which include single rotor [1], double rotors [2] surface-mounted PMSMs and interior PMSMs (IPMSMs) [3]. It is important to note that finite-element analysis (FEA) has been used to facilitate in searching for the optimum dimensions when designing the IPMSMs [3]. Meanwhile, the semi-analytical model using permeance function to estimate the airgap flux density was proposed in determining the optimal design of one segmented PM [1] and *n*th segmented PMs [4] per magnet pole in the surface-mounted PMSMs. Additionally, the magnetic lumped circuits could also be explored to predict the performance of surface-mounted PMSMs [2]. However, the analytical models in predicting the performances of the machines are superior to FEA because of the latter approach is requires significantly long computational time, especially during the design search for optimum performance of PMSMs.

The advantages such as simple construction, low cost and light weight which can be found in single-rotor surface-mounted PMSMs motivate the authors' interest in UV applications. In this paper, we present a fast computation subdomain model of the segmented magnets per pole in two-dimensional (2D) semi-closed surface-mounted PMSMs by using virtual PM blocks, where the prediction is more accurate than that of the semi-analytical model [5]. The motor performances such as the cogging torque and the total harmonic distortion (THD_v) of phase back-EMF are calculated. Next, the optima setting of one segmented magnet pole-arc and two segmented magnet pole-arcs are determined after normalizing the peak cogging torque and the THD_v. Finally, the FEA results are used to validate the analytical results of the optimum machines.

2 Machine Specifications and Assumptions

Figure 1 shows the geometric representation of a three-phase surface-mounted PM machine with segmented magnets per pole. The motor specifications are listed in Table 1. The parameters are defined as the inner radius of rotor yoke R_r, the radius of PM surface R_m, the inner and outer radii of slot-openings, R_s and R_t, respectively, the radius of the bottom slots R_{sb}, the magnet thickness h_m, the airgap length l_g, the slot-openings angle b_{oa}, the slot width angle b_{sa}, the winding slot width angle d_j, the current density J_i, the initial rotor position α_0, the rotor rotational speed ω_r, the position of the ith slot as the ith slot machine confined in four regions, i.e., Region

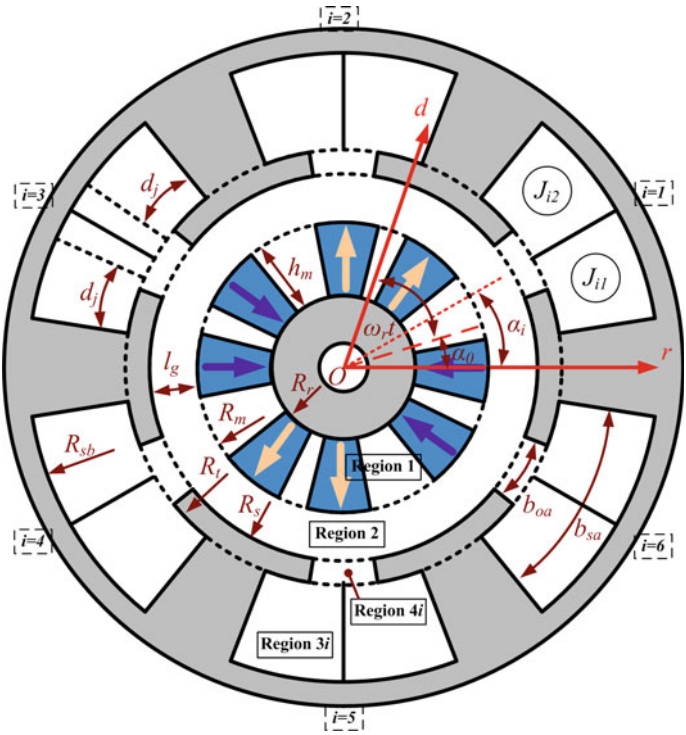

Fig. 1 Symbols and four regions (Region 1: PM, Region 2: airgap, Region 3*i*: the *i*th winding slot, Region 4*i*: the *i*th slot-opening) of a three-phase surface-mounted PM machine

Table 1 Specifications of the PM Machine

Parameters	6 s/4p	Parameters	6 s/4p	Parameters	6 s/4p
Slot number, N_s	6	Winding turns/coil	40	Stator outer diameter	66 mm
Pole number, $2p$	4	Tooth-tips edge	3 mm	Stator inner diameter	30 mm
Remanence, B_r	1.12 T	Slot-opening angle	10° mech	Rotor outer diameter	28 mm
Active length	50 mm	Winding slot angle	32° mech	Magnet thickness	3 mm
Airgap length	1 mm	Stator yoke height	8 mm	Relative recoil permeability, μ_r	1.05

1: PM, Region 2: airgap, Region 3*i*: the *i*th winding slot, Region 4*i*: the *i*th slot-opening. Furthermore, the assumptions for deriving the analytical model can be found in [5].

3 Subdomain Model with Segmented Magnets and Optimum Parametric Evaluation

The magnetic vector potentials in the PM A_{z1}, airgap A_{z2}, winding slots A_{z3i}, and slot-openings A_{z4i}, are governed by

$$\partial^2 A_{z1}/\partial r^2 + \partial A_{z1}/(r\partial r) + \partial^2 A_{z1}/\left(r^2\partial\alpha^2\right) = -(\mu_0/r)(M_\alpha - \partial M_r/\partial\alpha) \quad (1)$$

$$\partial^2 A_{z2}/\partial r^2 + \partial A_{z2}/(r\partial r) + \partial^2 A_{z2}/\left(r^2\partial\alpha^2\right) = 0 \quad (2)$$

$$\partial^2 A_{z3i}/\partial r^2 + \partial A_{z3i}/(r\partial r) + \partial^2 A_{z3i}/\left(r^2\partial\alpha^2\right) = -\mu_0 J \quad (3)$$

$$\partial^2 A_{z4i}/\partial r^2 + \partial A_{z4i}/(r\partial r) + \partial^2 A_{z4i}/\left(r^2\partial\alpha^2\right) = 0 \quad (4)$$

where M_r and M_α are the radial and tangential components of magnet magnetization. Figure 2 illustrated the segmented magnets per pole by virtual PM blocks. As can be seen, the total airgap flux density of the segmented magnets is modeled by adding the individual flux density produced by v-pieces of virtual PM blocks. The fluxes from each virtual PM block can be superimposed, assuming no saturation effects occur, therefore, the flux density of the segmented magnets per pole can be attained. So, the Fourier Series for the segmented magnets per magnetic pole with radial magnetization (RM) patterns can be expressed as

$$M_r = \sum_k^\infty M_{rk}\cos(k\alpha_r) \text{ for } k = up = 1, 3, 5, \ldots \quad (5)$$

$$M_\alpha = \sum_k^\infty M_{\alpha k}\sin(k\alpha_r) \text{ for } k = up = 1, 3, 5, \ldots \quad (6)$$

$$\text{while } M_{rk} = \sum_{v=1,2,3,\ldots}(-1)^{(v+1)}(4pB_r/k\pi\mu_0)\sin\left(k\pi\alpha_{pv}/2p\right), k/p = 1, 3, 5, \ldots \quad (7)$$

$$M_{\alpha k} = 0 \quad (8)$$

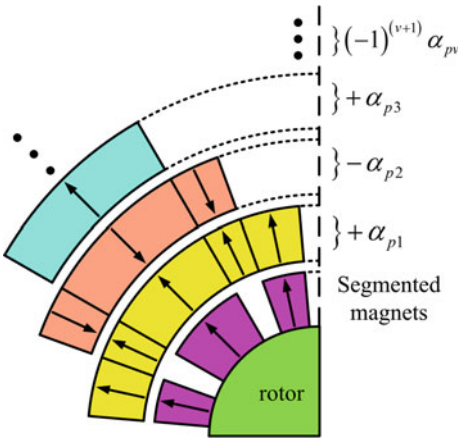

Fig. 2 Modeling of the typical segmented magnets per pole by virtual PM blocks

where u is the PM harmonic number, p is the pole-pair number, α_r is the rotor position, B_r is the PM remanence, α_{pv} is the magnet pole-arc ratio of v-pieces of virtual PM blocks, M_{rk} and $M_{\alpha k}$ are the kth harmonic of the radial and tangential components of magnetization vector. Then, a field solutions set can be obtained by solving the magneto-quasi equations in each subdomains using separable variable technique [5].

The global quantities for the motor can be calculated after having the field solutions set, which include the phase back-EMF, the cogging torque, and the THD_v to evaluate the performance of the surface-mounted PM machines. The formulations can be obtained in **Appendix**. The flux linkages of a non-overlapping windings with two coil sides of J_{i1} and J_{i2}, are obtained by (9) and (10), respectively, where l_a is the active axial length, N_c is the number of turns per coil, n is the harmonic number in the winding slot, A_c is the area of one coil side, while E_n, Z_0 and Z_n can be obtained in [5]. The total flux linkage of each individual phases can be calculated by (11), which is then further computed for phase back-EMF by using (12), where S_w is the matrix representing the winding arrangements in the stator slots, ψ_c is the flux linkage in every single coil side, and Δ is the rotor position. In addition, the THD_v of phase back-EMF can be evaluated by (13), where V_x is the RMS voltage of the xth harmonic and V_1 is the RMS voltage of the fundamental frequency. On the other hand, the cogging torque can be calculated by (14) where coefficients B_{2r} and $B_{2\alpha}$ are given in [5]. Therefore, the peak cogging torque can be found. The peak cogging torque and the THD_v of the phase back-EMF are normalized according to the feature scaling method, which is computed as in (15), where y_{in} is the normalized value of y_i, y_i is the ith value of y, and y is the data sample for either the peak cogging torque or the THD_v of the phase back-EMF. Eventually, the optimum setting of the magnet arcs required by the segmented magnets in the machines can be obtained.

4 Results, Discussion, and FEA Validation

In this paper, a generic, 6-slot/4pole (6 s/4p), three-phase surface-mounted PMSM is investigated to search for the optima design of the magnet pole-arcs, which is suitable for UVs applications. The main parameters of the PM machine are given in Table 1. Figure 3 shows the normalized peak cogging torque and the normalized THD_v when the magnet pole-arc is varied in 6 s/4p PM machine having either one segmented magnet (1SM) per magnetic pole or two-segmented magnets (2SM) per magnetic pole. From Fig. 3a, the optimum magnet pole-arc of 1SM is 135.7° elect., which can generate the peak cogging torque and THD_v of 0.052 Nm and 6.81 %, respectively. Then, by selecting the same PM volume as a constraint, we varied the magnet spans of the virtual PM blocks to determine the best segmented magnet pole-arcs using the proposed analytical model, potentially leads to lower the cogging torque and THD_v. Similar normalized waveforms can be observed in Fig. 3b when the magnet pole-arc α_{p1} is varied from 135.7° elect. to 180° elect., which

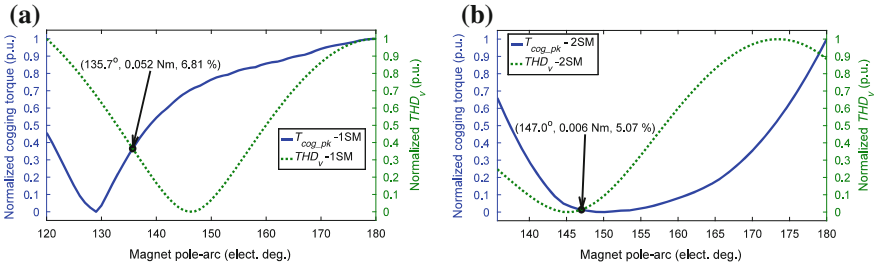

Fig. 3 The normalized peak cogging torque and the normalized total harmonic distortion of the phase back-EMF when the magnet pole-arc is varied in the 6 s/4p PM machine with each magnet pole of **a** 1SM **b** 2SM

corresponds to changes of the magnet pole-arc α_{p2} from 0° elect. to 44.3° elect. It is noted that significantly low cogging torque (0.006 Nm) and THD_v (5.07 %) are predicted from the optimum setting for the 2SM per magnet pole pertaining to α_{p1} of 147.0° elect. and α_{p2} of 11.3° elect. By comparing the cogging torque and THD_v produced by 1SM and 2SM per magnetic pole machines, both parameters have been intensively reduced by 88 % and 26 %, respectively. The 2D FEA motor models are built for validation purposes. Figure 4 shows the analytical and FE predictions of the phase back-EMF and cogging torque in the 6 s/4p PM machine having the same PM volume with the optimum magnet pole-arc of 1SM and 2SM per magnetic pole. A good agreement is obtained between the analytical and FEA results. Hence, the optima setting of the segmented magnet pole-arcs can be determined rapidly by the proposed analytical subdomain model, which can include the segmented magnets formulated by virtual PM blocks. The phase back-EMF waveform is prone to be more sinusoidal; while, the cogging torque can be minimized to a significantly low value. So, the 2SM per magnetic pole machine is well suited as a prime mover for the UV applications.

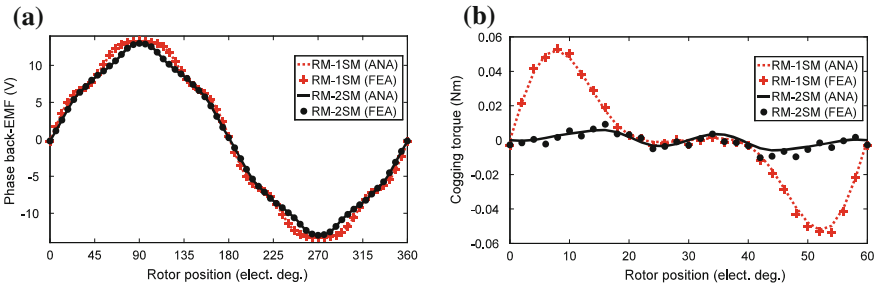

Fig. 4 Analytical and FE predictions in the 6 s/4p PM machines having the same PM volume with the optimum magnet pole-arcs in each magnet pole of 1SM and 2SM pertaining to **a** the phase back-EMF **b** the cogging torque

5 Conclusion

An analytical subdomain model of using virtual PM blocks to represent the segmented magnets per magnetic pole in two-dimensional (2D) semi-closed surface-mounted PMSMs is developed especially for UV applications. The analytical model is utilized in assisting, searching, and determining the optima magnet pole-arcs of 1SM and 2SM per magnetic pole under the influence of radial magnetization patterns in a three-phase, 6 s/4p surface-mounted PMSM. Normalization through feature scaling method is imposed on the peak cogging torque and the THD_v of phase back-EMF to discover the optimum PM pole-arc. From the investigation, the optimum magnet pole-arc of 135.7° elect. is able to produce the peak cogging torque and THD_v of phase back-EMF of 0.052 Nm and 6.81 %, respectively, by the 1SM per magnetic pole machine. Taking PM volume as the constraint, the optimum setting for the 2SM pole-arcs is evaluated to be 147.0° elect. per magnet pole associated with 11.3° elect. of airgap spacing between two magnet segments, which is predicted to generate the peak cogging torque and THD_v of phase back-EMF of 0.006 Nm and 5.07 %, respectively. Remarkably, the optimum design of 2SM per magnetic pole machine exhibits better performances as compared with that of 1SM per magnetic pole machine, where the cogging torque and THD_v have been reduced by 88 % and 26 %, respectively. The FEA results show good agreement with the analytical results as can be seen from the performances validation of both optimum PM machines.

Appendix 1

$$\psi_{i1} = (l_a N_c / A_c)\left[Z_0 d_j + \sum_n (Z_n / E_n) \sin\left(E_n d_j\right)\right] \tag{9}$$

$$\psi_{i2} = (l_a N_c / A_c)\left[Z_0 d_j - \sum_n (Z_n / E_n) \sin\left(n\pi - E_n d_j\right)\right] \tag{10}$$

$$\Psi_{abc} = S_w \psi_c \tag{11}$$

$$E_{abc} = \omega_r (d\Psi_{abc} / d\Delta) \tag{12}$$

$$THD_v = \left(\sqrt{\sum_{x=2}^{\infty} V_x^2} / V_1\right) \times 100 \tag{13}$$

$$T_c = \left(l_a r^2 / \mu_0\right) \int_0^{2\pi} B_{2r} B_{2\alpha} d\alpha \tag{14}$$

$$y_{in} = \frac{y_i - \min(y)}{\max(y) - \min(y)} \tag{15}$$

References

1. Ilka RS, Gholamian A (2012) Optimum design of a five-phase permanent magnet synchronous motor for underwater vehicles by use of particle swarm optimization. Telkomnika 10:715–724
2. Jinhua C, Fengge Z, Guangwei L, Zhaohe M (2009) Design and finite element analysis on a novel PMSM with anti-rotation dual rotor. In: IEEE international conference on automation and logistics 2009 (ICAL 2009), pp 315–319. IEEE Press, New York
3. Youlong W, Wen X, Lei Z, Zhang J (2011) Design and experimental verification of high power density interior permanent magnet motors for underwater propulsions. In: International conference on electrical machines and systems 2011 (ICEMS 2011), pp 1–6. IEEE Press, New York
4. Ashabani M, Mohamed YARI (2011) Multiobjective shape optimization of segmented pole permanent-magnet synchronous machines with improved torque characteristics. IEEE Trans Magn 47:795–804
5. Tiang TL, Ishak D, Lim CP, Jamil MKM (2015) A comprehensive analytical subdomain model and its field solutions for surface-mounted permanent magnet machines. IEEE Trans Magn 51:1–14